Challenge Journal of Structural Mechanics

Analytical solution for bending and buckling response of laminated non-homogeneous plates using a simplified-higher order theory

Ferruh Turan *, Muhammed Fatih Başoğlu, Zihni Zerin

Department of Civil Engineering, Ondokuz Mayıs University, 55139 Samsun, Turkey

ABSTRACT

In this study, analytical solutions for the bending and buckling analysis of simply supported laminated non-homogeneous composite plates based on first and simplified-higher order theory are presented. The simplified-higher order theory assumes that the in-plane rotation tensor is constant through the thickness. The constitutive equations of these theories were obtained by using principle of virtual work. Numerical results for the bending response and critical buckling loads of cross-ply laminates are presented. The effect of non-homogeneity, lamination schemes, aspect ratio, side-to-thickness ratio and in-plane orthotropy ratio on the bending and buckling response were analysed. The obtained results are compared with available elasticity and higher order solutions in the literature. The comparison studies show that simplified-higher order theory can achieve the same accuracy of the existing higher order theory for non-homogeneous thin plate.

ARTICLE INFO

Article history:
Received 12 January 2017
Accepted 16 February 2017

Keywords:
bending response
buckling response
shear deformation
higher-order theory
non-homogeneous plates
non-homogeneity effect

1. Introduction

Laminated composite plates are used in air craft industry, defense industry and especially structural strengthening applications. Usage of composite plates have been expanded due to their light-weight, high stiffness and high strength features compared to classical structural materials. For using them efficiently in above fields, their structural and dynamical behavior and also an accurate knowledge of their characteristic behaviors under various loading and boundary conditions are requested (Patel, 2014; Sadoune et al., 2014; Zerin et al., 2016).

Kinematic approaches for first-order shear deformation theory (FSDT) are an extension of the classical plate theory by including linear transverse shear deformation occurred through the plate thickness. However, the classical elasticity theory represents that transverse shear stress is distributed parabolically through the plate thickness. Because of that, FSDT requires a shear correction factor (K) to modify this parabolic shear stress distribution. Higher-order shear deformation theories (HSDTs) contain higher order variations of the displacement through the thickness and perform the equilibrium conditions obtained from elasticity theory on the top and bottom surface of the plate without using any shear correction factors.

Materials are generally considered as homogeneous and isotropic in classical elasticity theory because of simplicity in calculation. On the contrary, material anisotropic properties should be included to be able to obtain more accurate and sensitive analysis results. However, number of elastic constants increase in an anisotropic body. In such a body should be analysed by utilizing anisotropic elasticity theory in order to determine stress and strain (Kolpakov, 1999; Lal, 2007).

The linear elasticity theory of non-homogeneous materials is based on Hooke Law, and material elastic properties differ functionally through the thickness of the plate. This is more realistic in terms of mathematical and physical modeling. In this case, the physical characteristic of the material changes point to point continually and it becomes the continuous function of the point coordinates (Beena and Parvathy, 2014; Fares and Zenkour, 1999; He et al., 2013; Kolpakov, 1999; Leknitskii and Fern, 1963; Schmitz and Horst, 2014; Sofiyev and

* *Corresponding author*. Tel.: +90-362-3121919 ; E-mail address: ferruh.turan@omu.edu.tr (F. Turan)
ISSN: 2149-8024 / DOI: https://doi.org/10.20528/cjsmec.2017.02.001

Kuruoglu, 2014; Sofiyev et al., 2008; Stürzenbecher and Hofstetter, 2011; Zenkour and Fares, 1999).

A new simple first order shear deformation theory almost the same as CLPT was derived in terms of parameters such as equation of motion and boundary conditions (Thai and Choi, 2013a). Lots of theories acceptable for homogeneous laminated plates were modified into the behaviours of buckling and free vibration of non-homogeneous rectangle plates. The effects of non-homogeneity and thickness ratio on natural vibration and critical buckling load were determined. In this study, it is expressed that CLPT is not convenient method to investigate the structural behaviours of non-homogeneous plates (Fares and Zenkour, 1999). The non-homogeneity effects on free vibration of non-homogeneous isotropic circular plates of non-linear thickness were analysed. The non-homogeneity was related to variation of Young's modulus and density of plate material (Gupta et al., 2006). The non-homogeneity behaviours of non-homogeneous rectangle plates were pointed out by means of small parameter method, and the effects of non-homogeneity and material anisotropy on deflection and stress values were evaluated (Zenkour and Fares, 1999).

Zenkour (2011) investigated bending of exponentially graded sandwich plate by using HSDT and Sinusoidal Shear Deformation Theory (SSDT) and Zenkour et al. (2007) presented an exact solution for linear bending analysis of non-homogeneous variable thickness orthotropic plates. Librescu and Khdeir (1988) analysed stresses and displacements of symmetric cross-ply laminated elastic plates using HSDT. Gupta et al. (2007) presented variations of vibration based on thermal effects at non-homogeneous orthotropic rectangular plate having parabolically varying thickness. Kim et al. (2009) suggested a two variable refined plate theory without using shear correction factor for laminated composite plates. Fares and Zenkour (1999) analysed the buckling and free vibration response of non-homogeneous plates with various plate theories, and they deduced that non-homogeneity effect on the plate stability is significant. Neves and Ferreira (2016) examined the free vibration and buckling problem of composite plate using by global meshless method. Vescovini and Dozio (2016) developed an approximate method to analyse the vibration and buckling problem of plates. The method based on Ritz solution and a variable kinematic approach. Yu et al. (2016) investigated the thermal buckling for functionally graded plates (FGPs) with internal cracks using a new numerical method based on the first-order shear deformation theory. They assumed that the mechanical properties of FGPs varied through the thickness as a power function. Mojahedin et al. (2016) analysed the stability problem of functionally graded circular plate consisted of porous materials using higher-order plate theory. They assumed that the porosity varies as a function through the thickness. Saheb and Aruna (2015) developed a coupled displacement field method to investigate the buckling response of moderately thick plates. Komur and Sonmez (2015) analysed the effect of cut-outs or openings on the plate stability. They assumed that perforated plates may lose their stability under axial compression. So, they considered perforated square and rectangular plates to study the buckling behavior of plates using finite element method. Sreehari and Maiti (2015) developed a finite element formulation for buckling and post-buckling response of laminated composite plates. This formulation based on inverse hyperbolic shear deformation theory and satisfied that non-linear shear stress distributions and zero shear stress on the top and bottom surfaces of the plate. Papkov and Banerjee (2015) presented a new method to analyse the free vibration and buckling problems of rectangular orthotropic plates. They simplified the boundary value problem by developing the superposition principle. So, the exact results for free vibration and buckling of orthotropic plates can be practically obtained by using this method. Kulkarni et al. (2015) investigated bending and buckling behavior of FGPs by using inverse trigonometric shear deformation theory. The material properties of plates considered as an exponential variation through the thickness. Reddy et al. (2015) studied the buckling analysis of FGPs had variable material properties through the thickness. They investigated the thickness stretching effect on the buckling of plates and the study considered non-zero shear stress on the top and bottom surfaces of plates.

2. Mathematical Model

Consider a fiber – reinforced rectangular laminated plate with aspect ratio a/b and total thickness h and, consisted of N orthotropic non-homogeneous layers with orientation angles $\theta_1, \theta_2, \ldots, \theta_N$ as shown in Fig. 1. The coordinate system is assumed that the middle plane of the plate coincides with xy plane, and z axis is perpendicular to the middle plane.

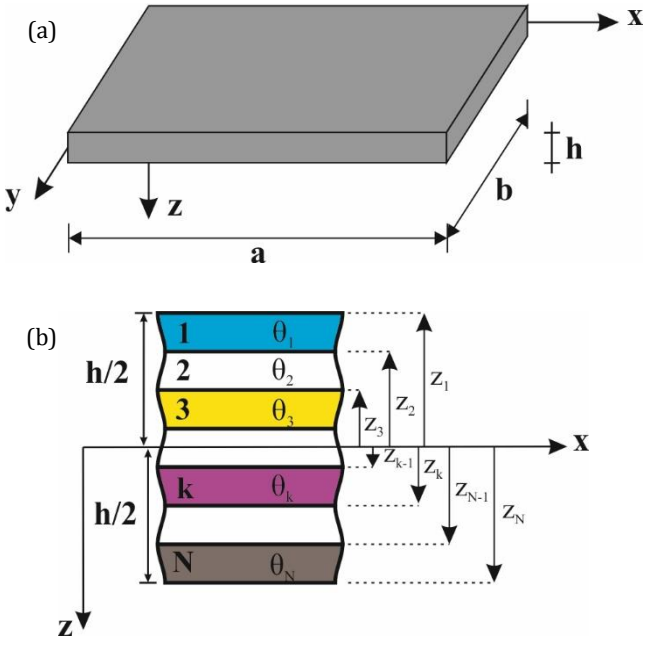

Fig. 1. Coordinate system (a) and lamination scheme (b) used for a typical laminate.

The first- and simplified higher-order theories used in the present study is based on the following displacement field (Reddy, 2004; Senthilnathan et al., 1988);

$$u(x,y,z) = u_0(x,y) - z\left[\alpha\frac{\partial w^b}{\partial x} - \beta\varphi_x + \gamma\frac{4z^2}{3h^2}\frac{\partial w^s}{\partial x}\right],$$

$$v(x,y,z) = v_0(x,y) - z\left[\alpha\frac{\partial w^b}{\partial y} - \beta\varphi_y + \gamma\frac{4z^2}{3h^2}\frac{\partial w^s}{\partial y}\right],$$

$$w(x,y,z) = \beta\, w + \alpha\, w^b + \gamma\, w^s, \quad (1)$$

where (u_0, v_0, w) are the displacement functions of the plate's mid-plane, ϕ_x and ϕ_y are the slopes in the xz and yz planes by reason of bending only and (α, β, γ) are arbitrary coefficients defined as;

1. Higher-order shear deformation theory (HSDT):
$\alpha = 1, \beta = 0, \gamma = 1.$
2. First-order shear deformation theory (FSDT):
$\alpha = 0, \beta = 1, \gamma = 0.$

In this study, simplified Reddy's theory is considered for HSDT. This theory is assumed that the slopes in the xz and yz planes (ϕ_x and ϕ_y) remains constant through the thickness and the transverse displacement w can be divided into bending (w^b) and shear (w^s) parts (Senthilnathan et al., 1988);

$$\frac{\partial\varphi_x}{\partial y} = \frac{\partial\varphi_y}{\partial x} \quad , \quad w = w^b + w^s \quad , \quad \varphi = -\nabla w^b . \quad (2)$$

The strains for FSDT and HSDT related to the displacements (1) can be presented as (Fares and Zenkour, 1999; Mojahedin et al., 2016; Reddy et al., 2015; Senthilnathan et al., 1988; Shahbaztabar and Ranji, 2016; Zenkour, 2011; Zenkour and Fares, 1999);

$$\varepsilon_{xx} = \varepsilon_{xx}^{(0)} + z\varepsilon_{xx}^{(1)} + z^3\varepsilon_{xx}^{(3)},$$

$$\varepsilon_{yy} = \varepsilon_{yy}^{(0)} + z\varepsilon_{yy}^{(1)} + z^3\varepsilon_{yy}^{(3)},$$

$$\varepsilon_{xy} = \varepsilon_{xy}^{(0)} + z\varepsilon_{xy}^{(1)} + z^3\varepsilon_{xy}^{(3)},$$

$$\varepsilon_{yz} = \varepsilon_{yz}^{(0)} + z^2\varepsilon_{yz}^{(2)},$$

$$\varepsilon_{xz} = \varepsilon_{xz}^{(0)} + z^2\varepsilon_{xz}^{(2)}, \quad (3)$$

where

$$\varepsilon_{xx}^{(0)} = \frac{\partial u_0}{\partial x}, \quad \varepsilon_{yy}^{(0)} = \frac{\partial v_0}{\partial y}, \quad \varepsilon_{xy}^{(0)} = \frac{\partial u_0}{\partial y} + \frac{\partial v_0}{\partial x},$$

$$\varepsilon_{yz}^{(0)} = \beta\left(\varphi_y + \frac{\partial w}{\partial y}\right) + \gamma\frac{\partial w^s}{\partial y},$$

$$\varepsilon_{xz}^{(0)} = \beta\left(\varphi_x + \frac{\partial w}{\partial x}\right) + \gamma\frac{\partial w^s}{\partial x},$$

$$\varepsilon_{xx}^{(1)} = -\alpha\frac{\partial^2 w^b}{\partial x^2} + \beta\ \frac{\partial\varphi_x}{\partial x},$$

$$\varepsilon_{yy}^{(1)} = -\alpha\frac{\partial^2 w^b}{\partial y^2} + \beta\ \frac{\partial\varphi_y}{\partial y},$$

$$\varepsilon_{xy}^{(1)} = -2\alpha\frac{\partial^2 w^b}{\partial x\partial y} + \beta\left(\frac{\partial\varphi_x}{\partial y} + \frac{\partial\varphi_y}{\partial x}\right),$$

$$\varepsilon_{xz}^{(2)} = -\gamma\frac{4}{h^2}\frac{\partial w^s}{\partial x},$$

$$\varepsilon_{yz}^{(2)} = -\gamma\frac{4}{h^2}\frac{\partial w^s}{\partial y}, \ \varepsilon_{xx}^{(3)} = -\gamma\frac{4}{3h^2}\frac{\partial^2 w^s}{\partial x^2},$$

$$\varepsilon_{yy}^{(3)} = -\gamma\frac{4}{3h^2}\frac{\partial^2 w^s}{\partial y^2}, \ \varepsilon_{xy}^{(3)} = -2\gamma\frac{4}{3h^2}\frac{\partial^2 w^s}{\partial x\partial y}. \quad (4)$$

The material elastic properties of the non-homogeneous laminates can be expressed as;

$$E_{11}^{(k)}(z) = E_{01}^{(k)}\left[1 + \mu\, f^{(k)}(z)\right],$$

$$E_{22}^{(k)}(z) = E_{02}^{(k)}\left[1 + \mu\, f^{(k)}(z)\right],$$

$$G_{12}^{(k)}(z) = G_{012}^{(k)}\left[1 + \mu\, f^{(k)}(z)\right],$$

$$G_{13}^{(k)}(z) = G_{013}^{(k)}\left[1 + \mu\, f^{(k)}(z)\right],$$

$$G_{23}^{(k)}(z) = G_{023}^{(k)}\left[1 + \mu\, f^{(k)}(z)\right],$$

$$max\left|\mu f^{(k)}(z)\right| < 1 \ , \ (k = 1, 2, \ldots, N) \ , \ f^{(k)}(z) = z \ , \quad (5)$$

where $E_{01}^{(k)}$, $E_{02}^{(k)}$, $G_{012}^{(k)}$, $G_{013}^{(k)}$ and $G_{23}^{(k)}$ are the material elastic properties of homogeneous orthotropic laminates. N is total laminate number, μ is a parameter that represents the variation of elasticity modulus through the plate thickness (non-homogeneous coefficient) and $f^{(k)}(z)$ is the continuous functions which express the variation of the elastic properties (Mojahedin et al., 2016; Reddy et al., 2015; Schmitz and Horst, 2014; Sofiyev, 2016; Sofiyev and Kuruoglu, 2014; Sofiyev and Kuruoğlu, 2016; Sofiyev et al., 2008).

In the shear deformation theory (SDT), stress-strain expressions of kth non-homogeneous laminate can be given as (Gosling and Polit, 2014; Mojahedin et al., 2016; Reddy et al., 2015; Reddy, 2004; Thai and Choi, 2013a; Zenkour, 2011; Zhen and Lo, 2015);

$$\begin{Bmatrix}\sigma_{xx}\\ \sigma_{yy}\\ \sigma_{yz}\\ \sigma_{xz}\\ \sigma_{xy}\end{Bmatrix}^{(k)} = \begin{bmatrix}\overline{Q}_{11} & \overline{Q}_{12} & 0 & 0 & \overline{Q}_{16}\\ \overline{Q}_{12} & \overline{Q}_{22} & 0 & 0 & \overline{Q}_{26}\\ 0 & 0 & \overline{Q}_{44} & \overline{Q}_{45} & 0\\ 0 & 0 & \overline{Q}_{45} & \overline{Q}_{55} & 0\\ \overline{Q}_{16} & \overline{Q}_{26} & 0 & 0 & \overline{Q}_{66}\end{bmatrix}^{(k)} \begin{Bmatrix}\varepsilon_{xx}\\ \varepsilon_{yy}\\ \varepsilon_{yz}\\ \varepsilon_{xz}\\ \varepsilon_{xy}\end{Bmatrix}^{(k)}, \quad (6)$$

where $\bar{Q}_{ij}$ are the transformed material properties expressed as (Fares, 1999; Reddy, 2004; Thai and Choi, 2013b; Zenkour and Fares, 1999; Zerin et al., 2016);

$$\bar{Q}_{11} = Q_{11}\cos^4\theta + Q_{22}\sin^4\theta + 2(Q_{12} + 2Q_{66})\sin^2\theta\cos^2\theta ,$$

$$\bar{Q}_{12} = (Q_{11} + Q_{22} - 4Q_{66})\sin^2\theta cos^2\theta + Q_{12}(\sin^4\theta + \cos^4\theta),$$

$$\bar{Q}_{16} = (Q_{11} - Q_{12} - 2Q_{66})\sin\theta\cos^3\theta + (Q_{12} - Q_{22} + 2Q_{66})\sin^3\theta\cos\theta ,$$

$$\bar{Q}_{22} = Q_{11}\sin^4\theta + Q_{22}\cos^4\theta + 2(Q_{12} + 2Q_{66})\sin^2\theta\cos^2\theta \;\; ; \;\; \bar{Q}_{55} = Q_{44}\sin^2\theta + Q_{55}\cos^2\theta ,$$

$$\bar{Q}_{26} = (Q_{11} - Q_{12} - 2Q_{66})\cos\theta\sin^3\theta + (Q_{12} - Q_{22} + 2Q_{66})\cos^3\theta\sin\theta ,$$

$$\bar{Q}_{44} = Q_{44}\cos^2\theta + Q_{55}\sin^2\theta ,$$

$$\bar{Q}_{45} = (Q_{55} - Q_{44})\cos\theta\sin\theta ,$$

$$\bar{Q}_{55} = Q_{44}\sin^2\theta + Q_{55}\cos^2\theta ,$$

$$\bar{Q}_{66} = (Q_{11} + Q_{22} - 2Q_{12} - 2Q_{66})\sin^2\theta\cos^2\theta + Q_{66}(\sin^4\theta + \cos^4\theta) , \tag{7}$$

in which θ is the angle between global x-axis and local x-axis of each laminate. The material properties of the laminate $Q_{\mathrm{ij}}^{(k)}$ are given by;

$$Q_{11}^{(k)} = \frac{E_{01}^{(k)}[1+\mu f^{(k)}(z)]}{1-\nu_{12}^{(k)}\nu_{21}^{(k)}} \;\; , \;\; Q_{12}^{(k)} = \frac{\nu_{12}^{(k)}E_{02}^{(k)}[1+\mu f^{(k)}(z)]}{1-\nu_{12}^{(k)}\nu_{21}^{(k)}} \;\; , \;\; Q_{22}^{(k)} = \frac{E_{02}^{(k)}[1+\mu f^{(k)}(z)]}{1-\nu_{12}^{(k)}\nu_{21}^{(k)}} \;\; ,$$

$$Q_{66}^{(k)} = G_{012}^{(k)}[1+\mu f^{(k)}(z)] \;\; , \;\; Q_{44}^{(k)} = G_{023}^{(k)}[1+\mu f^{(k)}(z)] \;\; , \;\; Q_{55}^{(k)} = G_{013}^{(k)}[1+\mu f^{(k)}(z)] \;\; , \tag{8}$$

where $E_{01}^{(k)}$ and $E_{02}^{(k)}$ are modulus of elasticity of homogeneous case in 1 and 2 material-principal directions, respectively; $G_{012}^{(k)}$, $G_{013}^{(k)}$ and $G_{023}^{(k)}$ are shear modulus of homogeneous case in the 1-2, 1-3 and 2-3 surfaces, respectively and v_{ij} are Poisson's ratio.

3. Equations of Motion

To obtain the equation of motion, the principle of virtual work are written as;

$$0 = \int_A \left\{\int_{-h/2}^{h/2}\left[\sigma_{xx}^{(k)}\left(\delta\varepsilon_{xx}^{(0)} + z\delta\varepsilon_{xx}^{(1)} + z^3\delta\varepsilon_{xx}^{(3)}\right) + \sigma_{yy}^{(k)}\left(\delta\varepsilon_{yy}^{(0)} + z\delta\varepsilon_{yy}^{(1)} + z^3\delta\varepsilon_{yy}^{(3)}\right) + \cdots\right]dz\right\} dxdy - \int_A q\delta\,(w^b + w^s)dA , \tag{9}$$

or

$$0 = \int_A \left[N_{xx}\delta\varepsilon_{xx}^{(0)} + M_{xx}\delta\varepsilon_{xx}^{(1)} + P_{xx}\delta\varepsilon_{xx}^{(3)} + N_{yy}\delta\varepsilon_{yy}^{(0)} + M_{yy}\delta\varepsilon_{yy}^{(1)} + P_{yy}\delta\varepsilon_{yy}^{(3)} + N_{xy}\delta\varepsilon_{xy}^{(0)} + M_{xy}\delta\varepsilon_{xy}^{(1)} + P_{xy}\delta\varepsilon_{xy}^{(3)} + Q_x\delta\varepsilon_{xz}^{(0)} + R_x\delta\varepsilon_{xz}^{(2)} + Q_y\delta\varepsilon_{yz}^{(0)} + R_y\delta\varepsilon_{yz}^{(2)} - q\delta(w^b + w^s)\right] , \tag{10}$$

where N, M, Q are the stress resultants and P and R are the higher order stress resultants defined by;

$$\begin{Bmatrix} N_{\xi\eta} \\ M_{\xi\eta} \\ P_{\xi\eta} \end{Bmatrix} = \sum_{k=1}^{N}\int_{z_{k-1}}^{z_k}\sigma_{\xi\eta}^{(k)}\begin{Bmatrix} 1 \\ z \\ z^3 \end{Bmatrix}dz \quad , \quad \begin{Bmatrix} Q_\xi \\ R_\xi \end{Bmatrix} = \sum_{k=1}^{N}\int_{z_{k-1}}^{z_k}\sigma_{\xi z}^{(k)}\begin{Bmatrix} 1 \\ z^2 \end{Bmatrix}dz \; . \tag{11}$$

Note that ξ and η take the symbols x and y. Substituting Eq.(9) into Eq.(11) the stress resultants are obtained as (Phan and Reddy, 1985; Reddy, 1984; Reddy, 2004; Reissner, 1975; Thai and Choi, 2013a, 2013b; Yin et al., 2014);

$$\begin{Bmatrix} \{N_{\xi\eta}\} \\ \{M_{\xi\eta}\} \\ \{P_{\xi\eta}\} \end{Bmatrix} = \begin{bmatrix} [A] & [B] & [E] \\ [B] & [D] & [F] \\ [E] & [F] & [H] \end{bmatrix}\begin{Bmatrix} \{\varepsilon_{\xi\eta}^{(0)}\} \\ \{\varepsilon_{\xi\eta}^{(1)}\} \\ \{\varepsilon_{\xi\eta}^{(3)}\} \end{Bmatrix} \quad , \quad \begin{Bmatrix} \{Q_\xi\} \\ \{R_\xi\} \end{Bmatrix} = \begin{bmatrix} [A] & [D] \\ [D] & [F] \end{bmatrix}\begin{Bmatrix} \{\varepsilon_{\xi z}^{(0)}\} \\ \{\varepsilon_{\xi z}^{(2)}\} \end{Bmatrix} . \tag{12a}$$

where

$$\left(A_{ij}, B_{ij}, D_{ij}, E_{ij}, F_{ij}, H_{ij}\right) = \sum_{k=1}^{N}\int_{z_{k-1}}^{z_k}\bar{Q}_{ij}^{(k)}(1, z, z^2, z^3, z^4, z^6)\,dz \quad (i,j = 1,2,6) \; .$$

$$\left(A_{ij}, D_{ij}, F_{ij}\right) = \sum_{k=1}^{N}\int_{z_{k-1}}^{z_k}\bar{Q}_{ij}^{(k)}(1, z^2, z^4)\,dz \quad (i,j = 4,5) \; . \tag{12b}$$

4. Analytical Solution

The determination of transverse deflection and stresses are the fundamental process in the design of many constructional components. Non-homogeneous function and non-homogeneous coefficients are used to analyse the non-homogeneous laminated plate.

Boundary conditions of a simply supported rectangular plate are;

$$x = 0, a \quad , \; u = w = \varphi_x = 0 \; .$$

$$y = 0, b \quad , \; v = w = \varphi_y = 0 \; . \tag{13}$$

The considered transverse distribution load can be expanded in a double Fourier series

$$q(x,y) = \sum_{m=1,3,..}^{\infty} \sum_{n=1,3,..}^{\infty} Q_{mn} \sin\left(\frac{m\pi x}{a}\right) \sin\left(\frac{n\pi y}{b}\right), \tag{14}$$

and

$$Q_{mn} = \begin{cases} q_0 & \text{for sinusoidal load, } m = n = 1 \\ \frac{16q_0}{mn\pi^2} & \text{for uniform load, } m,n = 1,3,5,\ldots \end{cases}, \tag{15}$$

where q_0 represents the load at the center of the plate.

Navier approach is considered for the analytical solution of the problems. So, it can be assumed that;

$$\begin{Bmatrix} \beta w \\ \alpha w^b \\ \gamma w^s \\ \beta \varphi_x \\ \beta \varphi_y \end{Bmatrix} = \sum_{m=1}^{\infty} \sum_{n=1}^{\infty} \begin{Bmatrix} \beta \, W_{mn} \sin(\frac{m\pi x}{a}) \sin(\frac{n\pi y}{b}) \\ \alpha \, W^b_{mn} \sin(\frac{m\pi x}{a}) \sin(\frac{n\pi y}{b}) \\ \gamma \, W^s_{mn} \sin(\frac{m\pi x}{a}) \sin(\frac{n\pi y}{b}) \\ \beta \, X_{mn} \cos(\frac{m\pi x}{a}) \sin(\frac{n\pi y}{b}) \\ \beta \, Y_{mn} \sin(\frac{m\pi x}{a}) \cos(\frac{n\pi y}{b}) \end{Bmatrix}, \tag{16}$$

where $W_{mn}, X_{mn}, Y_{mn}, W^b_{mn}$ and W^s_{mn} are the arbitrary coefficients. Substituting Eqs. (4), (15a) and (16) into the Eq. (12) and substituting Eqs. (4), (12a) and (16) into the Eq. (9), we get for the bending problem;

$$[S]\{\Gamma_{mn}\} = \{F\}, \tag{17}$$

and for the buckling problem, we can get

$$([P] - [L])\{\Gamma_{mn}\} = \{0\}, \tag{18}$$

where

$$\{\Gamma_{mn}\} = \{\beta \, W_{mn} \quad \alpha \, W^b_{mn} \quad \gamma \, W^s_{mn} \quad \beta \, X_{mn} \quad \beta \, Y_{mn}\}^T, \tag{19}$$

is the solution vector. The elements of the coefficient matrices $[P]$, $[L]$ and $[S]$ are defined in Appendix A. For solution of Eq. (17), the following determinant should be zero and this equation gives the critical buckling loads;

$$|[P] - [L]| = 0 \, . \tag{20}$$

5. Numerical Results and Discussion

In this section, various numerical examples are analyzed and discussed to confirm the accuracy of the present study for bending and buckling analysis of non-homogeneous composite plates. For all problems a simply supported plate is considered for analysis. The transverse loading considered is sinusoidal for bending problems. Results of analysis are obtained in closed form using Navier's solution procedure for the above geometry and loading and the accuracy of the numerical results is confirmed by comparing results with their counterparts in the literature (Librescu and Khdeir, 1988; Noor, 1973; Pagano, 1970; Pagano and Hatfield, 1972; Putcha and Reddy, 1986; Reddy, 2004).

Note that Model-1, Model-2 and Model-3 represents the displacement fields of Zenkour and Fares (1999), simplified-higher order theory and first order theory, respectively, for bending analysis of plates. Displacement fields of simplified-higher order theory and first order theory is also considered for buckling analysis of the laminated plates. Also, shear correction factor is determined as $5/6$ for FSDT.

It is assumed that the thickness and the material are same for all laminates and the following sets of data and non-dimensionalizations are used to present results;

$Material\ 1\ (bending)$:

$$E_{01} = 25E_{02} \, , \;\; G_{012} = G_{013} = 0.5E_{02} \, ,$$

$$G_{023} = 0.2E_{02} \, , \;\; \nu_{12} = 0.25 \; .$$

$Material\ 2\ (buckling)$:

$$E_{01} = 40E_{02} \, , \;\; G_{012} = G_{013} = 0.6E_{02} \, ,$$

$$G_{023} = 0.5E_{02} \, , \;\; \nu_{12} = 0.25 \; . \tag{21}$$

and

$$\bar{w} = \frac{100h^3 E_{02}}{q_0 a^4} w\left(\frac{a}{2}, \frac{b}{2}\right) \, ,$$

$$\bar{\sigma}_x = \frac{h^2}{q_0 a^2} \sigma_x\left(\frac{a}{2}, \frac{b}{2}, \frac{h}{2}\right) \, ,$$

$$\bar{\sigma}_y = \frac{h^2}{q_0 a^2} \sigma_y\left(\frac{a}{2}, \frac{b}{2}, \frac{h}{4}\right) \, ,$$

$$\bar{\sigma}_{xy} = \frac{h^2}{q_0 a^2} \sigma_{xy}(0,0,-\frac{h}{2}) \, ,$$

$$\bar{\sigma}_{yz} = \frac{h}{q_0 a} \sigma_{yz}(\frac{a}{2}, 0, 0) \, ,$$

$$\bar{\sigma}_{xz} = \frac{h}{q_0 a} \sigma_{xz}(0, \frac{b}{2}, 0) \, ,$$

$$\bar{N}_{cr} = \frac{N_{cr} a^2}{E_{02} h^3} \, . \tag{22}$$

5.1. Example 1

A simply supported four-layered symmetric cross-ply ($0^0/90^0/90^0/0^0$) non-homogeneous rectangular plate subjected to sinusoidal transverse load is considered. The layers have equal thickness. The numerical results of deflection and stresses are given in Table 1.

The results show that the values obtained from HSDT (present) and Zenkour and Fares (1999) present good agreement based on increasing of a/h ratios. For a/h ratio equal to 4, deflection of Model-1 by 18.63%, Model-2 by 24.78%, Model-3 by 13.42% compared to the results of elasticity solution. Fig. 8 shows the variation of transverse displacement versus a/h ratios. It demonstrates that the results obtained from Model-2 and Model-3 are in good agreement by increasing a/h ratios and shows that transverse displacement values decrease based on increase of non-homogeneous coefficients. The results show that Model-2 gives better accuracy in thin plates (a/h=100) compared to other models whereas Model-1 gives better accuracy in thick plates (a/h=4). The in-plane stress values of all models increase with the increasing a/h ratios. Fig. 9 shows the variation of transverse displacement versus a/b ratios for a/h ratio equal to 10. It shows that the transverse displacement values obtained by using Model-2 and Model-3 are in excellent agreement for a/b ratio equal to 2 and shows that transverse displacement values decrease with increasing of non-homogeneous coefficients. Fig. 10 shows the variation of $\bar{\sigma}_x$ through the thickness of symmetric cross-ply ($0^0/90^0/90^0/0^0$) square plate for a/h ratio equal to 4. Figs. 11 and 12 contain similar plots of $\bar{\sigma}_{xz}$ and $\bar{\sigma}_{yz}$ for a/b ratio of 1 and 3 and a/h ratio equal to 4. They show that the stress values obtained by using Model-2 and Model-3 decrease with the increasing of non-homogeneous coefficients.

Table 1. Non-dimensionalized deflections and stresses in four-layer cross-ply (0/90/90/0) square laminates under sinusoidal transverse loads.

a/h	Source	$\bar{w}$	$\bar{\sigma}_x$	$\bar{\sigma}_y$	$\bar{\sigma}_{xz}$	$\bar{\sigma}_{yz}$	$\bar{\sigma}_{xy}$
	Elasticity	1.9540	0.7200	0.6630	0.2910	0.2920	0.0467
	Zenkour	1.8937	0.6651	0.6322	0.2064	0.2389	0.0440
	$\mu = 0.01$	1.5899	0.6345	0.6033	0.1834	0.2106	0.0372
4	HSDT (present)	1.4858	0.7584	0.1116	0.3312	0.1325	0.0300
	$\mu = 0.01$	1.4698	0.7503	0.1110	0.3310	0.1324	0.0302
	FSDT (present)	1.7101	0.4064	0.5410	0.3495	0.0785	0.0308
	$\mu = 0.01$	1.6917	0.4020	0.5361	0.3493	0.0784	0.0311
	Elasticity	0.7430	0.5590	0.4010	0.3010	0.1960	0.0275
	Zenkour	0.7147	0.5456	0.3888	0.2640	0.1531	0.0268
	$\mu = 0.01$	0.6049	0.5242	0.3711	0.2339	0.1352	0.0228
10	HSDT (present)	0.6046	0.5752	0.1634	0.3395	0.1358	0.0227
	$\mu = 0.01$	0.5981	0.5690	0.1624	0.3393	0.1357	0.0229
	FSDT (present)	0.6632	0.4994	0.3647	0.4165	0.0517	0.0242
	$\mu = 0.01$	0.6560	0.4941	0.3614	0.4162	0.0516	0.0244
	Elasticity	0.5170	0.5430	0.3080	0.3280	0.1560	0.0230
	Zenkour	0.5060	0.5393	0.3043	0.2825	0.1234	0.0228
	$\mu = 0.01$	0.4310	0.5187	0.2918	0.2499	0.1096	0.0195
20	HSDT (present)	0.4751	0.5483	0.1710	0.3408	0.1363	0.0217
	$\mu = 0.01$	0.4700	0.5424	0.1700	0.3405	0.1362	0.0219
	FSDT (present)	0.4916	0.5279	0.3108	0.4370	0.0435	0.0221
	$\mu = 0.01$	0.4863	0.5222	0.3079	0.4366	0.0434	0.0223
	Elasticity	0.4385	0.5390	0.2760	0.3370	0.1410	0.0216
	Zenkour	0.4343	0.5387	0.2708	0.2897	0.1117	0.0213
	$\mu = 0.01$	0.3713	0.5187	0.2605	0.2561	0.0995	0.0183
100	HSDT (present)	0.4334	0.5396	0.1734	0.3412	0.1365	0.0213
	$\mu = 0.01$	0.4288	0.5338	0.1724	0.3409	0.1364	0.0215
	FSDT (present)	0.4341	0.5388	0.1741	0.4448	0.0403	0.0213
	$\mu = 0.01$	0.4295	0.5330	0.1731	0.4445	0.0403	0.0215

5.2. Example 2

A simply supported three-layered symmetric cross-ply ($0^0/90^0/0^0$) non-homogeneous rectangular plate subjected to sinusoidal transverse load is considered. The layers have equal thickness. The numerical results of transverse displacement and stresses for various side-to-thickness ratios (a/h) and aspect ratio of 3 are given in Table 2. The results show that the values obtained from HSDT (present) and Zenkour and Fares (1999) display good agreement with increasing of a/h ratios. It is understood from the results that, the deflection and stresses diminish by increasing the non-homogeneity coefficient. This results imply that the laminated composite plate become more rigid due to inclusion of non-homogeneous elastic properties. The results show that the error achieved by using the Model-3 is very large compared to other models and the error reduces with increasing of slenderness ratio (a/h). For a/h equal to 4, 10 and 20, Model-2 gives better result of in-plane stress $\bar{\sigma}_x$ whereas Model-3 gives more accurate results of in-plane shear stress than the other models for the above side-to-thickness ratios. For very thin non-homogeneous plates (a/h=100) Model-2 gives more accurate results of $\bar{\sigma}_x$ and in-plane shear stress than the other models. Fig. 2 shows the variation of transverse displacements of

non-homogeneous laminated square plate versus side-to-thickness ratio and Fig. 3 shows the variation of transverse displacement of non-homogeneous laminated plate with aspect ratio for a/h=10. It can be seen from these figures that the transverse displacement values decrease with increasing of a/h ratios and non-homogeneous coefficients for both Model-2 and Model-3, and these values increase with increasing of a/b ratios for both Model-2 and Model-3. The transverse displacement value obtained by using Model-2 and Model-3 are in excellent agreement for a/h ratio of 10. It is understood from Figs. 3, 5 and 7 that the effect of non-homogeneity is substantial for rectangular plates due to high aspect ratio, while it becomes less remarkable for symmetric and antisymmetric square plates. Fig. 4 shows that the discrepancy of in-plane stress $\bar{\sigma}_y$ between Model-2 and Model-3 diminish by increasing of a/h ratio and Fig. 5 shows that the variation of in-plane stress $\bar{\sigma}_y$ is minimum for aspect ratio of 3 for both Model-2 and Model-3. Figs. 6 and 7 shows that the discrepancy of in-plane shear stress between Model-2 and Model-3 diminish with increasing of a/h and a/b ratios for side-to-thickness ratio of 10.

Table 2. Non-dimensionalized deflections and stresses in rectangular (a=3b), three-layer cross-ply (0/90/0) laminates under sinusoidal transverse loads.

a/h	Source	$\bar{w}$	$\bar{\sigma}_x$	$\bar{\sigma}_y$	$\bar{\sigma}_{xz}$	$\bar{\sigma}_{yz}$	$\bar{\sigma}_{xy}$
	Elasticity	2.8200	1.1000	0.1190	0.3870	0.0334	0.0281
	Zenkour	2.6411	1.0356	0.1028	0.0348	0.2724	0.0263
	$\mu = 0.01$	2.2148	0.9884	0.0971	0.2414	0.0314	0.0221
4	HSDT (present)	3.1942	1.1541	0.0255	0.8522	0.1136	0.0154
	$\mu = 0.01$	3.1599	1.1417	0.0253	0.8515	0.1135	0.0155
	FSDT (present)	2.3631	0.6095	0.0054	0.4698	0.0123	0.0205
	$\mu = 0.01$	2.3378	0.6030	0.0054	0.4694	0.0123	0.0207
	Elasticity	0.9190	0.7250	0.0435	0.4200	0.0152	0.0123
	Zenkour	0.8622	0.6924	0.0398	0.0170	0.2859	0.0115
	$\mu = 0.01$	0.7309	0.6664	0.0380	0.2531	0.0155	0.0098
10	HSDT (present)	0.9560	0.7121	0.0392	0.8951	0.1193	0.0095
	$\mu = 0.01$	0.9458	0.7045	0.0389	0.8944	0.1192	0.0096
	FSDT (present)	0.8035	0.6204	0.0354	0.4735	0.0064	0.0105
	$\mu = 0.01$	0.7949	0.6138	0.0351	0.4731	0.0064	0.0106
	Elasticity	0.6100	0.6500	0.0299	0.4340	0.0119	0.0093
	Zenkour	0.5937	0.6407	0.0289	0.0139	0.2880	0.0091
	$\mu = 0.01$	0.5073	0.6180	0.0278	0.2529	0.0128	0.0078
20	HSDT (present)	0.6177	0.6453	0.0413	0.9016	0.1202	0.0086
	$\mu = 0.01$	0.6111	0.6384	0.0410	0.9008	0.1201	0.0087
	FSDT (present)	0.5789	0.6222	0.0403	0.4741	0.0054	0.0088
	$\mu = 0.01$	0.5727	0.6156	0.0400	0.4737	0.0054	0.0089
	Elasticity	0.5080	0.6240	0.0253	0.4390	0.0108	0.0083
	Zenkour	0.5077	0.6240	0.0253	0.2886	0.0129	0.0083
	$\mu = 0.01$	0.4350	0.6024	0.0244	0.2555	0.0119	0.0071
100	HSDT (present)	0.5085	0.6238	0.0420	0.9037	0.1205	0.0083
	$\mu = 0.01$	0.5030	0.6171	0.0417	0.9029	0.1204	0.0084
	FSDT (present)	0.5069	0.6228	0.0419	0.4743	0.0051	0.0083
	$\mu = 0.01$	0.5015	0.6162	0.0416	0.4739	0.0051	0.0084

5.3. Example 3

A simply supported three- and four-layered symmetric cross-ply non-homogeneous rectangular plate subjected to biaxial or uniaxial compressive load is considered. Tables 3 and 4 present the dimensionless critical buckling loads of cross-ply square plates for orthotropy ratios (E_1/E_2) and for various values of non-homogeneity coefficient μ. It can be seen that the present numerical results of critical buckling loads for the homogeneous (μ=0) plates obtained through the present HSDT are in good agreement with the corresponding results above. The discrepancy between critical buckling loads predicted by FSDT and HSDT increases with increase of non-homogeneity coefficients. The numerical results show that the critical buckling loads increase with increasing of the orthotropy ratio of individual layer and non-homogeneity coefficient. Furthermore, the number of layers has not a significant effect on critical buckling loads. Figs. 13 and 14 show that the results of critical buckling load obtained through the present theories are in good agreement for orthotropy ratio of 16, and Tables 3 and 4 confirm that HSDT gives more accurate results than FSDT compared to Three-dimensional elasticity solution and higher-order theory solution. Figs. 15-17 illustrate the variation of the dimensionless critical buckling loads versus the plate side-to-thickness ratio and the plate aspect ratio, respectively. It can be seen in corresponding figures that the non-homogeneity effect is more significant in thin (high side-to-thickness ratio) laminated plates with high aspect ratio. This means that the plate stability is strengthened with increasing these ratios. Figs. 18 and 19 display the variation of the dimensionless critical buckling loads vs. compressing ratio (k) for (0/90/0) and (0/90/90/0) square plates. These figures represent that the non-homogeneity effect on the stability process is weak for high ratios of (k) and a/h.

Table 3. Non-homogeneity effects on the biaxial critical buckling loads ($\bar{N}_{cr} = N_{cr}a^2/E_{02}h^3$) of (0/90/0) square plates (a/h=10, k=1).

E_1/E_2	Khdeir & Librescu	$\mu = 0.00$		$\mu = 0.02$		$\mu = 0.04$	
		FSDT	HSDT	FSDT	HSDT	FSDT	HSDT
2	2.3640	2.9279	2.3076	2.9913	2.3576	3.0548	2.4076
10	4.9630	5.4722	5.0925	5.5908	5.2028	5.7094	5.3131
20[a]	5.5160	7.9683	7.8343	8.1410	8.004	8.3136	8.1738
30[a]	9.0560	9.5439	9.4369	9.7507	9.6414	9.9574	9.8459
40[a]	10.2590	10.7091	10.8887	10.9411	11.1246	11.1732	11.3605

[a] The lowest critical buckling occurs at mode numbers m=1 , n=2, otherwise the critical buckling occurs at mode numbers m=1, n=1.

Table 4. The effect of the orthotropy on the uniaxial buckling load ($\bar{N}_{cr} = N_{cr}a^2/E_{02}h^3$) of cross-ply square plates (a/h=10, k=0).

Source	Lamination scheme	E_1/E_2				
		3	10	20	30	40
Putcha & Reddy	0/90/0	5.3933	9.9406	15.2980	19.6740	23.3400
Noor		5.3044	9.7621	15.0191	19.3040	22.8807
Zenkour		5.3899	9.8325	14.8896	18.8776	22.1207
$\mu = 0.05$		5.5635	10.0866	15.2113	19.2358	22.4985
HSDT (present)		5.3526	10.1849	16.2233	21.4351	25.9817
$\mu = 0.05$		5.6425	10.7366	17.1021	22.5962	27.389
FSDT (present)		6.5594	10.9445	15.9366	19.8796	23.0869
$\mu = 0.05$		6.9147	11.5373	16.7999	20.9564	24.3374
Reddy	0/90/90/0	5.1140	9.7770	15.2980	19.9570	23.3400
Noor		5.3040	9.7620	15.0190	19.3040	22.8810
HSDT (present)		5.3526	10.1849	16.2233	21.4351	25.9817
$\mu = 0.05$		5.6425	10.7366	17.1021	22.5962	27.389
FSDT (present)		6.5612	11.0325	16.2911	20.5926	24.2037
$\mu = 0.05$		6.9166	11.6301	17.1736	21.708	25.5147

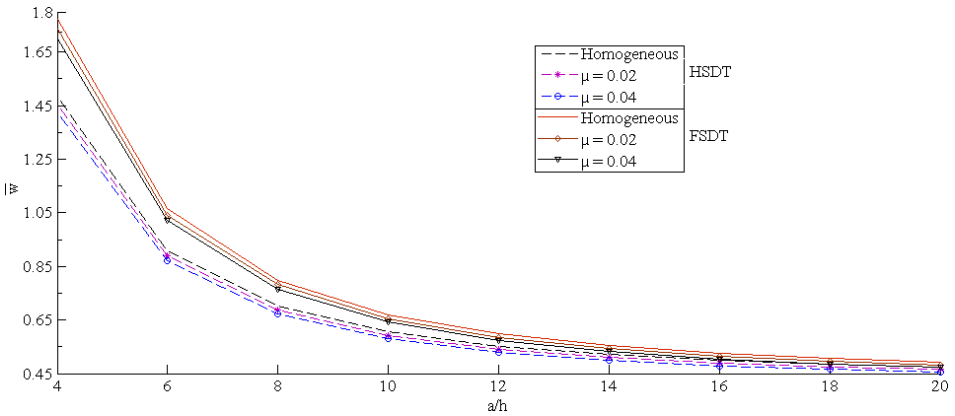

Fig. 2. Non-dimensional center deflection ($\bar{w}$) versus side-to-thickness ratio of a (0/90/0) square plate under sinusoidal load for various values of μ.

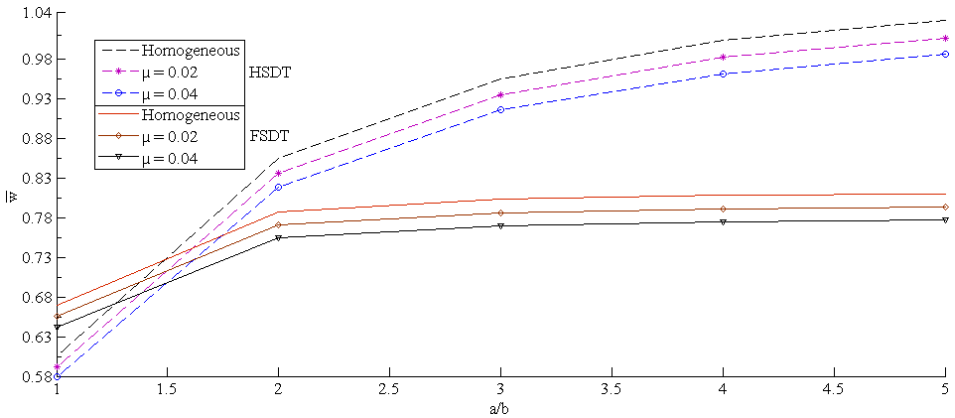

Fig. 3. Effect of the aspect ratio on the center deflection ($\bar{w}$) of a (0/90/0) plate under sinusoidal load for various values of μ ($a/h = 10$).

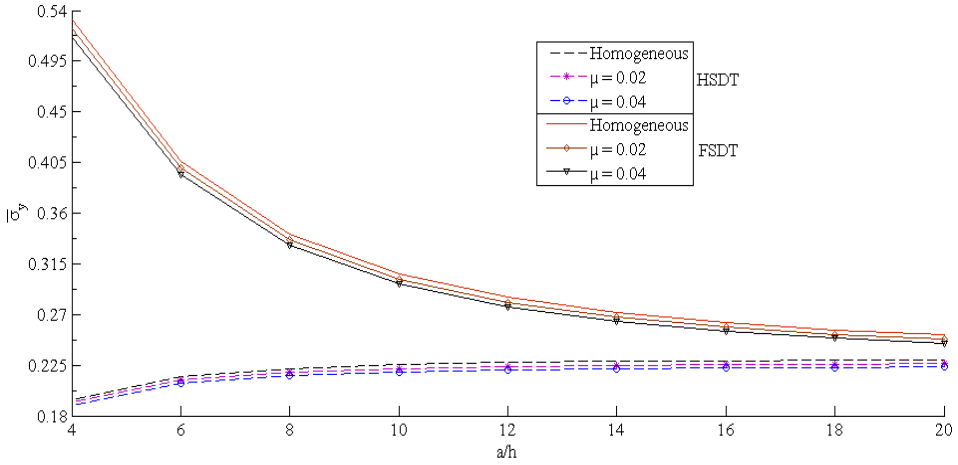

Fig. 4. Non-dimensional normal stress ($\bar{\sigma}_y$) versus side-to-thickness ratio of a (0/90/0) plate under sinusoidal load for various values of μ.

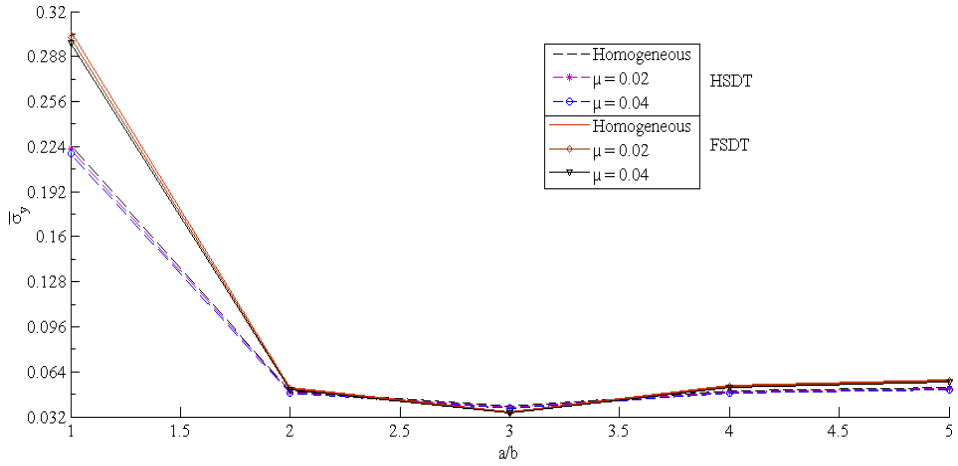

Fig. 5. Effect of the aspect ratio on the normal stress ($\bar{\sigma}_y$) of a (0/90/0) plate under sinusoidal load for various values of μ ($a/h = 10$).

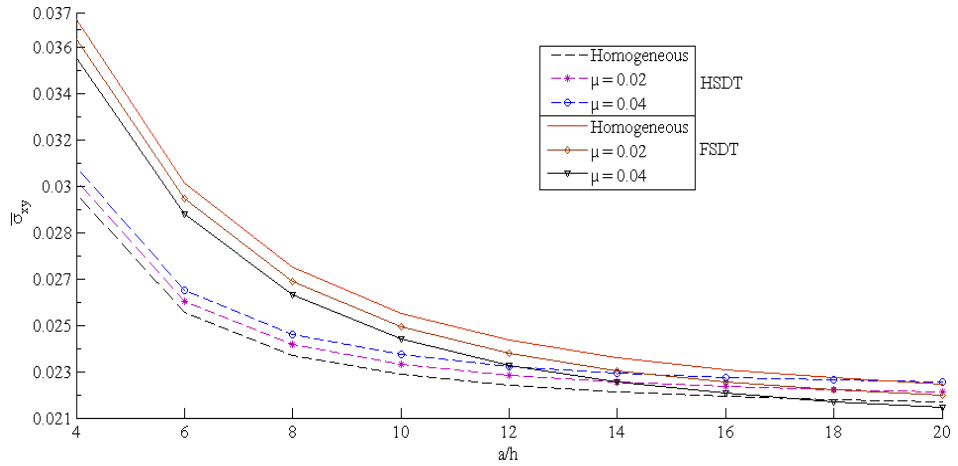

Fig. 6. Non-dimensional tangential stress ($\bar{\sigma}_{xy}$) versus side-to-thickness ratio of a (0/90/0) square plate under sinusoidal load for various values of μ.

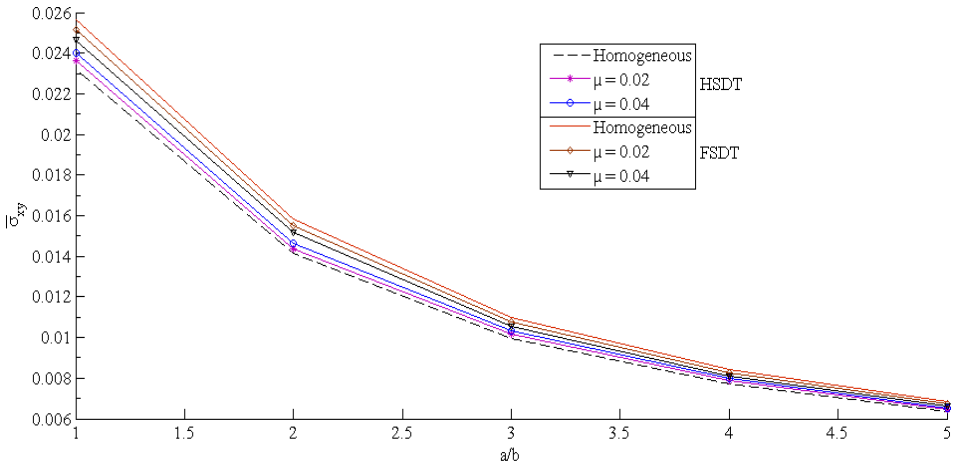

Fig. 7. Effect of the aspect ratio on the tangential stress ($\bar{\sigma}_{xy}$) of a (0/90/0) plate under sinusoidal load for various values of μ ($a/h = 10$).

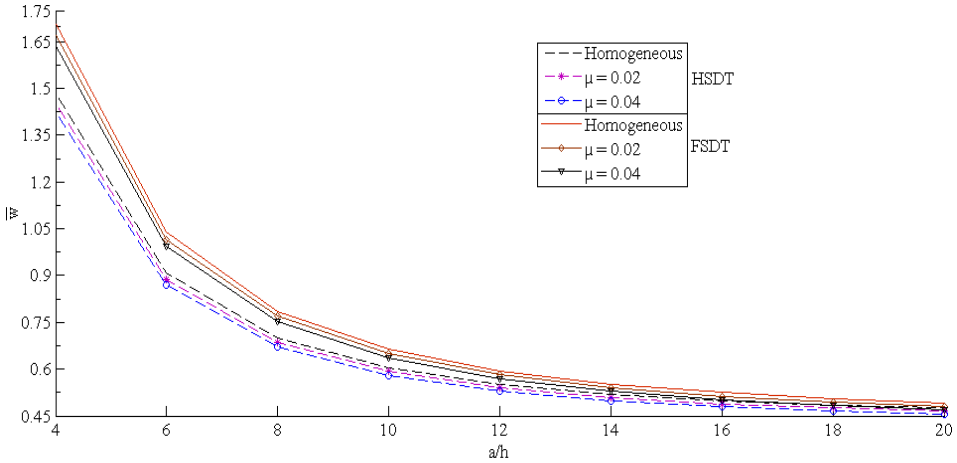

Fig. 8. Non-dimensional center deflection ($\bar{w}$) versus side-to-thickness ratio of a (0/90/90/0) square plate under sinusoidal load for various values of μ.

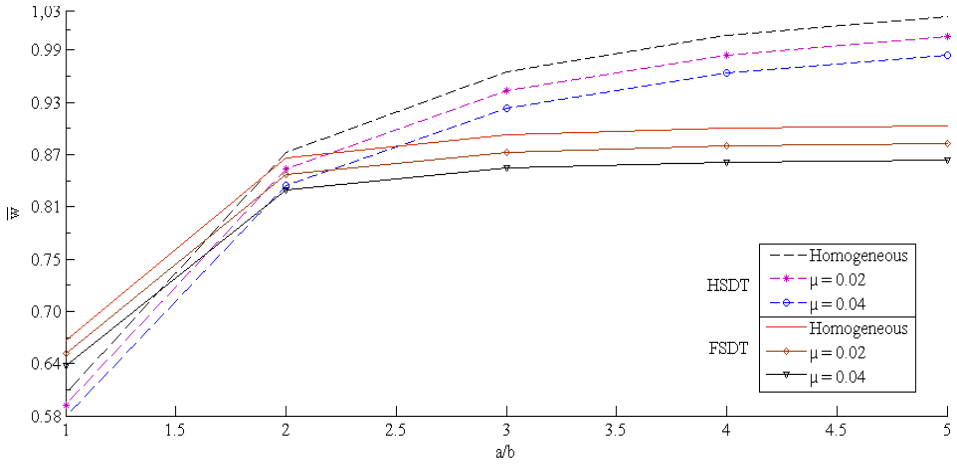

Fig. 9. Effect of the aspect ratio on the center deflection ($\bar{w}$) of a (0/90/90/0) plate under sinusoidal load for various values of μ ($a/h = 10$).

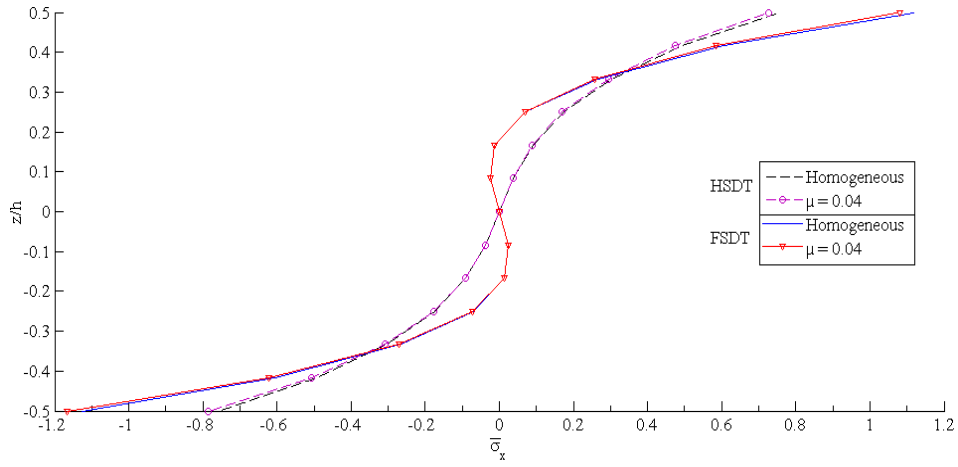

Fig. 10. Variation of non-dimensional normal stress ($\bar{\sigma}_x$) through the laminate thickness of a (0/90/90/0) square plate under sinusoidal load for various values of μ ($a/h = 4$).

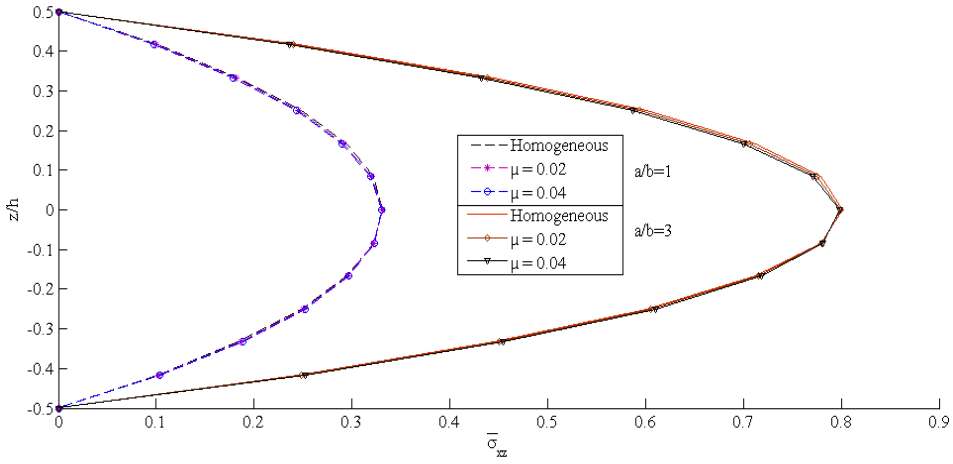

Fig. 11. Variation of non-dimensional normal stress ($\bar{\sigma}_{xz}$) through the laminate thickness of a (0/90/90/0) square plate under sinusoidal load for various values of μ ($a/h = 4$).

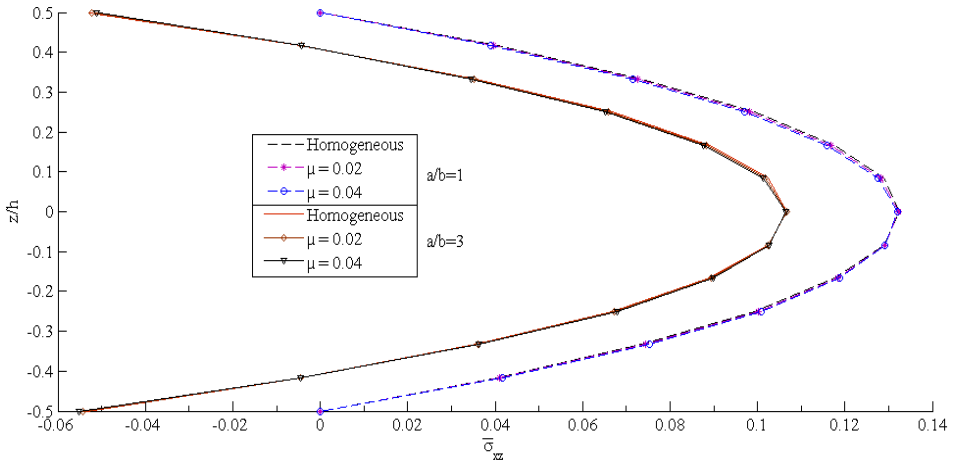

Fig. 12. Variation of non-dimensional normal stress ($\bar{\sigma}_{yz}$) through the laminate thickness of a (0/90/90/0) square plate under sinusoidal load for various values of μ ($a/h = 4$).

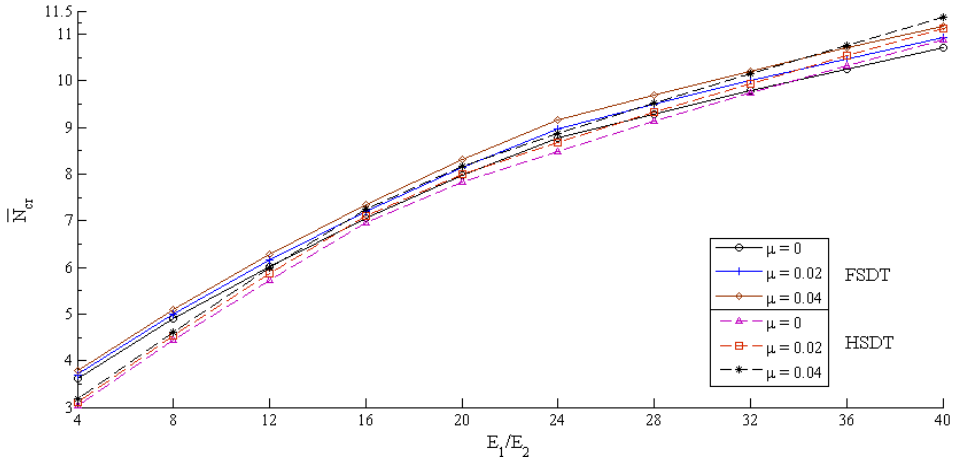

Fig. 13. Effect of the orthotropy ratio on the biaxial critical buckling load of a (0/90/0) square plate for various values of μ $(a/h = 10,\ k = 1)$.

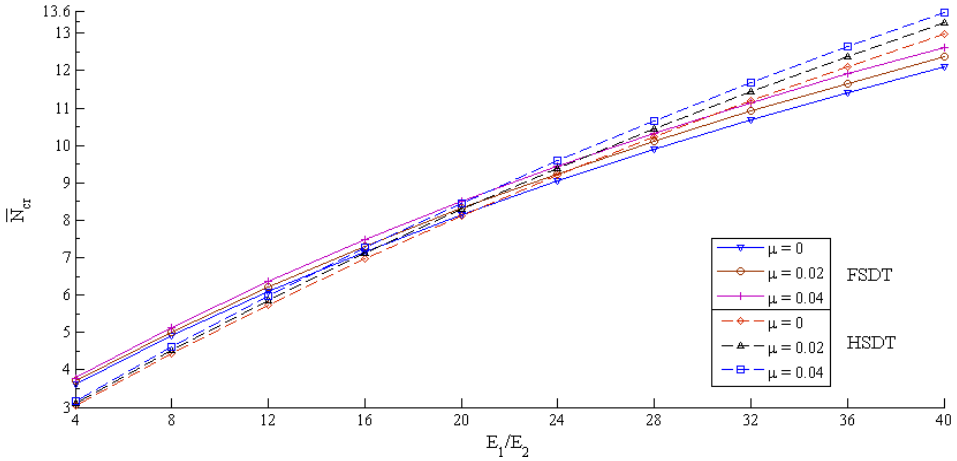

Fig. 14. Effect of the orthotropy ratio on the biaxial critical buckling load of a (0/90/90/0) square plate for various values of μ $(a/h = 10,\ k = 1)$.

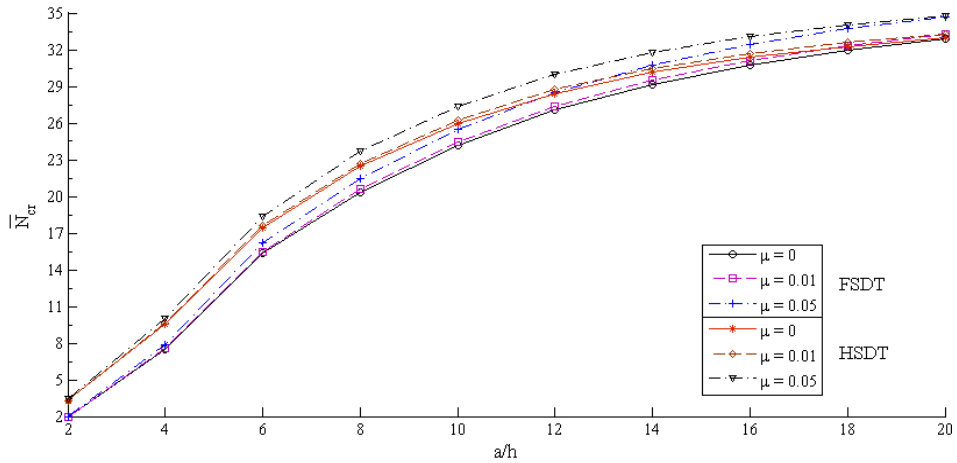

Fig. 15. Effect of the side-to-thickness ratio on the axial critical buckling load of a (0/90/90/0) square plate for various values of μ $(a/h = 10,\ k = 0)$.

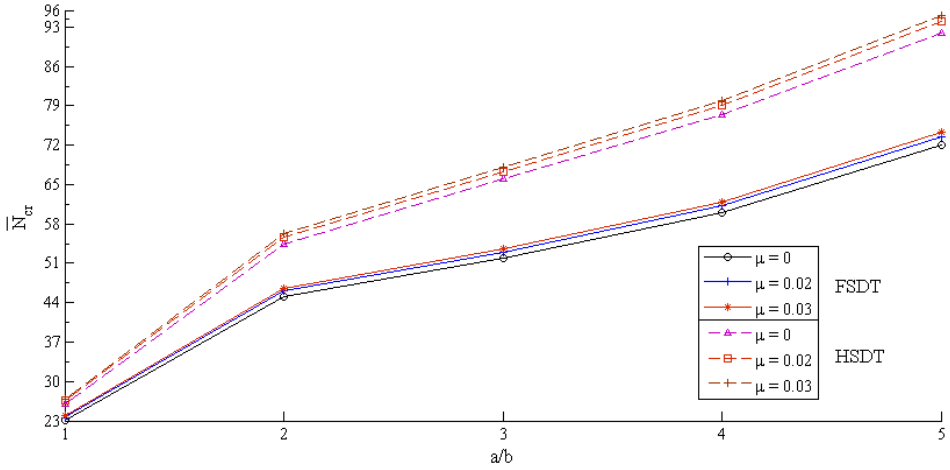

Fig. 16. Effect of the aspect ratio on the axial critical buckling load of a (0/90/0) plate for various values of μ $(a/h = 10,\ k = 0)$.

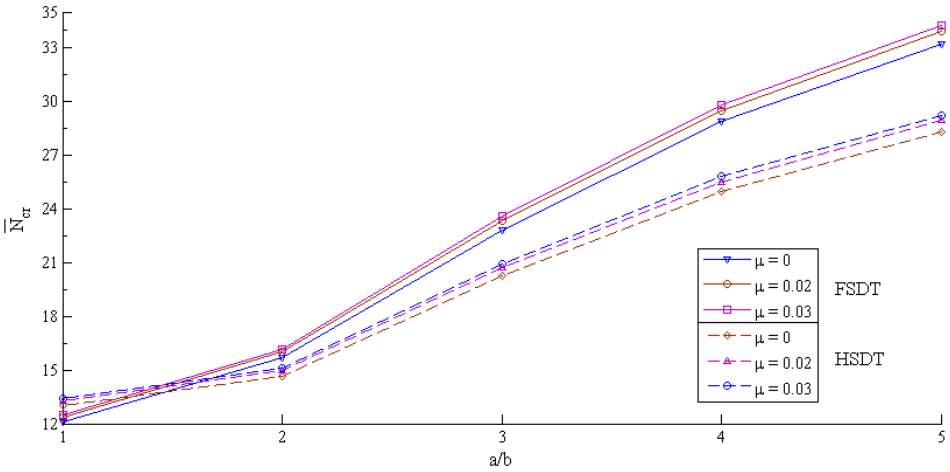

Fig. 17. Effect of the aspect ratio on the axial critical buckling load of a (0/90/90/0) plate for various values of μ $(a/h = 10,\ k = 1)$.

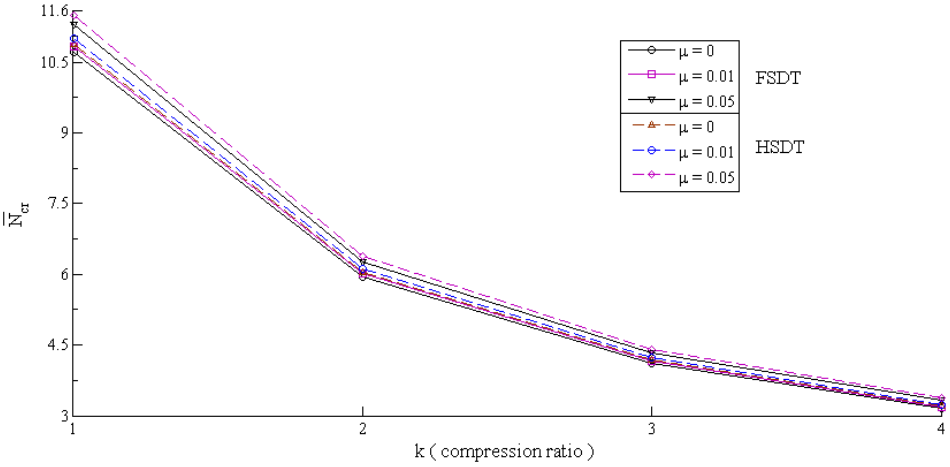

Fig. 18. Effect of the k (compression ratio) on the critical buckling load of a (0/90/0) square plate for various values of μ $(a/h = 10)$.

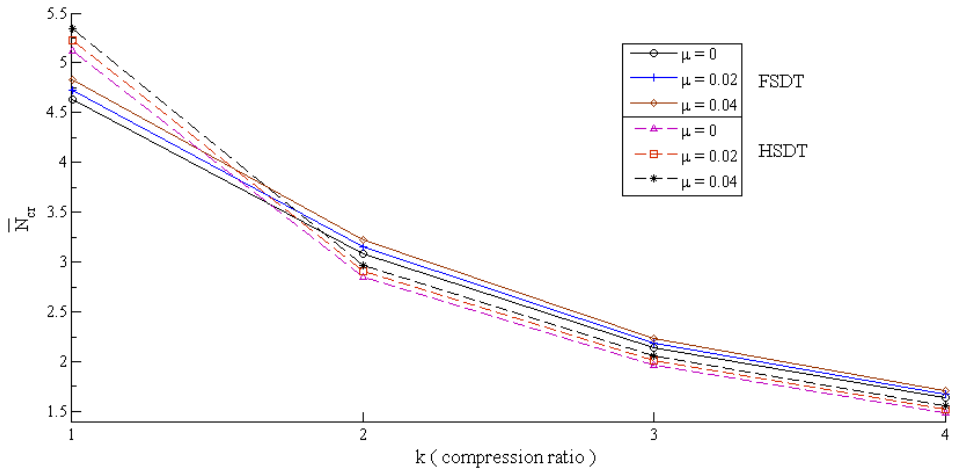

Fig. 19. Effect of the k (compression ratio) on the critical buckling load of a (0/90/90/0) square plate for various values of μ $(a/h = 4)$.

6. Conclusions

Analytical solutions for the bending analysis of simply supported laminated non-homogeneous composite plates based on first and simplified-higher order theory are presented. The displacement field of simplified-higher order theory assumes that the in-plane rotation tensor is constant through the thickness. For thin and very thin non-homogeneous laminated plates the solution of the simplified-higher order theory (Model-2) is found a good agreement with the elasticity solution and percentage error with respect to elasticity solution is much less compared to other shear deformation theories used for comparison in this study. For thick non-homogeneous laminated plates the results of Model-1 is in good agreement with the elasticity solution. The main aim of this study is to reveal the accuracy of the various shear deformation theory for bending analysis of non-homogeneous laminated plates.

The buckling problems of non-homogeneous rectangular plates are investigated. Numerical results for the critical buckling loads of symmetric cross-ply laminates are predicted by both of first- and higher-order theories. The effects of non-homogeneity, aspect ratio, side-to-thickness ratio, compressing ratio and in-plane orthotropy ratio on critical buckling loads are illustrated. The numerical results are compared with corresponding results similar studies. The study concludes that the present first- and higher-order theories predict reasonable accuracy the buckling response of non-homogeneous plates. Furthermore, the non-homogeneity, aspect ratio and in-plane orthotropy ratio have a significant effect on the stability process and buckling response of laminates.

Appendix A.

The elements $S_{ij} = S_{ji}$ of the coefficient matrix $[S]$:

$$S_{11} = K(A_{55}\lambda^2\beta^2 + A_{44}\mu^2\beta^2) \quad , \quad S_{12} = 0 \quad , \quad S_{13} = K(A_{55}\lambda^2\beta\gamma + A_{44}\mu^2\beta\gamma) - c_2\,(D_{55}\lambda^2\beta\gamma + D_{44}\mu^2\beta\gamma) \ ,$$

$$S_{14} = K\lambda\beta^2 A_{55} \quad , \quad S_{15} = K\mu\beta^2 A_{44} \quad , \quad S_{22} = \lambda^4\alpha^2 D_{11} + 2\lambda^2\mu^2\alpha^2(D_{12} + 2D_{66}) + \mu^4\alpha^2 D_{22} \ ,$$

$$S_{23} = c_1\lambda^4\alpha\gamma F_{11} + 2c_1\lambda^2\mu^2\alpha\gamma(F_{12} + 2F_{66}) + c_1\mu^4\alpha\gamma F_{22} \quad , \quad S_{24} = -\lambda^3\alpha\beta D_{11} - \lambda\mu^2\alpha\beta(D_{12} + 2D_{66}) \ ,$$

$$S_{25} = -\lambda^2\mu\alpha\beta(D_{12} + 2D_{66}) - \mu^3\alpha\beta D_{22} \ ,$$

$$S_{33} = c_1^2\lambda^4\gamma^2 H_{11} + 2c_1^2\lambda^2\mu^2\gamma^2(H_{12} + 2H_{66}) + c_1^2\mu^4\gamma^2 H_{22} + c_2^2(\lambda^2\gamma^2 F_{55} + \mu^2\gamma^2 F_{44}) - 2c_2(\lambda^2\gamma^2 D_{55} + \mu^2\gamma^2 D_{44}) + \lambda^2\gamma^2 A_{55} + \mu^2\gamma^2 A_{44} \ ,$$

$$S_{34} = -c_1(\lambda^3\beta\gamma F_{11} + \lambda\mu^2\beta\gamma(F_{12} + 2F_{66}) - c_2\lambda\beta\gamma D_{55} + K\lambda\beta\gamma A_{55} \ ,$$

$$S_{35} = -c_1(\lambda^2\mu\beta\gamma(F_{12} + 2F_{66}) + \mu^3\beta\gamma F_{22}) - c_2\mu\beta\gamma D_{44} + K\mu\beta\gamma A_{44} \ ,$$

$$S_{44} = \lambda^2\beta^2 D_{11} + \mu^2\beta^2 D_{66} + K\beta^2 A_{55} \ ,$$

$$S_{45} = \lambda\mu\beta^2(D_{12} + D_{66}), S_{55} = \mu^2\beta^2 D_{22} + \lambda^2\beta^2 D_{66} + K\beta^2 A_{44} \ ,$$

and the elements $P_{ij} = P_{ji}$ of the coefficient matrix $[P]$:

$$P_{11} = S_{11} + L_{11} \quad , \quad P_{12} = S_{12} + L_{12} \quad , \quad P_{13} = S_{13} + L_{13} \quad , \quad P_{14} = S_{14} \quad , \quad P_{15} = S_{15}, P_{22} = S_{22} + L_{22},$$

$$P_{23} = S_{23} + L_{23} \quad , \quad P_{24} = S_{24} \quad , \quad P_{25} = S_{25} \quad , \quad P_{33} = S_{33} + L_{33} \quad , \quad P_{34} = S_{34} \quad , \quad P_{35} = S_{35} \quad , \quad P_{44} = S_{44},$$

$$P_{45} = S_{45} \quad , \quad P_{55} = S_{55} \ .$$

where

$$L_{11} = N_0\lambda^2\beta^2 + kN_0\mu^2\beta^2 \quad , \quad L_{12} = N_0\lambda^2\alpha\beta + kN_0\mu^2\alpha\beta \quad , \quad L_{13} = N_0\lambda^2\beta\gamma + kN_0\mu^2\beta\gamma \ ,$$

$$L_{22} = N_0\lambda^2\alpha^2 + kN_0\mu^2\alpha^2 \quad , \quad L_{23} = N_0\lambda^2\alpha\gamma + kN_0\mu^2\alpha\gamma \quad , \quad L_{33} = N_0\lambda^2\gamma^2 + kN_0\mu^2\gamma^2 \ ,$$

$$\lambda = \frac{m\pi x}{a} \quad , \quad \mu = \frac{n\pi y}{b} \quad , \quad c_1 = \frac{4}{3h^2} \quad , \quad c_2 = -\frac{4}{h^2} \ ,$$

and K is shear correction factor and it is determined as $5/6$ for FSDT.

REFERENCES

Beena K, Parvathy U (2014). Linear static analysis of functionally graded plate using spline finite strip method. *Composite Structures,* 117, 309-315.

Fares M (1999). Non-linear bending analysis of composite laminated plates using a refined first-order theory. *Composite Structures,* 46(3), 257-266.

Fares M, Zenkour A (1999). Buckling and free vibration of non-homogeneous composite cross-ply laminated plates with various plate theories. *Composite Structures,* 44(4), 279-287.

Gosling P, Polit O (2014). A high-fidelity first-order reliability analysis for shear deformable laminated composite plates. *Composite Structures, 115*, 12-28.

Gupta A, Johri T, Vats R (2007). Thermal effect on vibration of non-homogeneous orthotropic rectangular plate having bi-directional parabolically varying thickness. *Proceeding of International Conference in World Congress on Engineering and Computer Science*.

Gupta U, Lal R, Sharma S (2006). Vibration analysis of non-homogeneous circular plate of nonlinear thickness variation by differential quadrature method. *Journal of Sound and Vibration,* 298(4), 892-906.

He WM, Chen WQ, Qiao H (2013). In-plane vibration of rectangular plates with periodic inhomogeneity: Natural frequencies and their adjustment. *Composite Structures,* 105, 134-140.

Kim S-E, Thai H-T, Lee J (2009). A two variable refined plate theory for laminated composite plates. *Composite Structures,* 89(2), 197-205.

Kolpakov A (1999). Variational principles for stiffnesses of a non-homogeneous plate. *Journal of the Mechanics and Physics of Solids,* 47(10), 2075-2092.

Komur MA, Sonmez M (2015). Elastic buckling behavior of rectangular plates with holes subjected to partial edge loading. *Journal of Constructional Steel Research,* 112, 54-60.

Kulkarni K, Singh B, Maiti D (2015). Analytical solution for bending and buckling analysis of functionally graded plates using inverse trigonometric shear deformation theory. *Composite Structures,* 134, 147-157.

Lal R (2007). Transverse vibrations of non-homogeneous orthotropic rectangular plates of variable thickness: A spline technique. *Journal of Sound and Vibration,* 306(1), 203-214.

Leknitskii SG, Fern P (1963). Theory of elasticity of an anisotropic elastic body. Holden-Day.

Librescu L, Khdeir A (1988). Analysis of symmetric cross-ply laminated elastic plates using a higher-order theory: Part I—Stress and displacement. *Composite Structures,* 9(3), 189-213.

Mojahedin A, Jabbari M, Khorshidvand A, Eslami M (2016). Buckling analysis of functionally graded circular plates made of saturated porous materials based on higher order shear deformation theory. *Thin-Walled Structures,* 99, 83-90.

Neves A, Ferreira A (2016). Free vibrations and buckling analysis of laminated plates by oscillatory radial basis functions. *Curved and Layered Structures, 3*(1), 17-21.

Noor AK (1973). Free vibrations of multilayered composite plates. *AIAA Journal,* 11(7), 1038-1039.

Pagano N (1970). Exact solutions for rectangular bidirectional composites and sandwich plates. *Journal of Composite Materials, 4*(1), 20-34.

Pagano N, Hatfield HJ (1972). Elastic behavior of multilayered bidirectional composites. *AIAA Journal,* 10(7), 931-933.

Papkov S, Banerjee J (2015). A new method for free vibration and buckling analysis of rectangular orthotropic plates. *Journal of Sound and Vibration,* 339, 342-358.

Patel SN (2014). Nonlinear bending analysis of laminated composite stiffened plates. *Steel and Composite Structures,* 17(6), 867-890.

Phan N, Reddy J (1985). Analysis of laminated composite plates using a higher-order shear deformation theory. *International Journal for Numerical Methods in Engineering,* 21(12), 2201-2219.

Putcha N, Reddy J (1986). Stability and natural vibration analysis of laminated plates by using a mixed element based on a refined plate theory. *Journal of Sound and Vibration,* 104(2), 285-300.

Reddy BS, Kumar JS, Reddy C, Reddy KVK (2015). Buckling analysis of functionally graded plates using higher order shear deformation theory with thickness stretching effect. *International Journal of Applied Science and Engineering* 13 (1*)*, 19-36.

Reddy JN (1984). A simple higher-order theory for laminated composite plates. *Journal of Applied Mechanics,* 51(4), 745-752.

Reddy JN (2004). Mechanics of laminated composite plates and shells: theory and analysis. CRC press.

Reissner E (1975). On transverse bending of plates, including the effect of transverse shear deformation. *International Journal of Solids and Structures,* 11(5), 569-573.

Sadoune M, Tounsi A, Houari MSA, Bedia ELAA (2014). A novel first-order shear deformation theory for laminated composite plates. *Steel and Composite Structures,* 17(3), 321-338.

Saheb KM, Aruna K (2015). Buckling analysis of moderately thick rectangular plates using coupled displacement field method. Journal of Physics: Conference Series.

Schmitz A, Horst P (2014). A finite element unit-cell method for homogenised mechanical properties of heterogeneous plates. *Composites Part A: Applied Science and Manufacturing,* 61, 23-32.

Senthilnathan N, Lim S, Lee K, Chow S (1988). Vibration of laminated orthotropic plates using a simplified higher-order deformation theory. *Composite Structures,* 10(3), 211-229.

Shahbaztabar A, Ranji AR (2016). Effects of in-plane loads on free vibration of symmetrically cross-ply laminated plates resting on Pasternak foundation and coupled with fluid. *Ocean Engineering,* 115, 196-209.

Sofiyev A (2016). Buckling of heterogeneous orthotropic composite conical shells under external pressures within the shear deformation theory. *Composites Part B: Engineering,* 84, 175-187.

Sofiyev A, Kuruoglu N (2014). Combined influences of shear deformation, rotary inertia and heterogeneity on the frequencies of cross-ply laminated orthotropic cylindrical shells. *Composites Part B: Engineering,* 66, 500-510.

Sofiyev A, Kuruoğlu N (2016). The stability of FGM truncated conical shells under combined axial and external mechanical loads in the framework of the shear deformation theory. *Composites Part B: Engineering,* 92, 463-476.

Sofiyev A, Zerin Z, Korkmaz A (2008). The stability of a thin three-layered composite truncated conical shell containing an FGM layer subjected to non-uniform lateral pressure. *Composite Structures,* 85(2), 105-115.

Sreehari V, Maiti D (2015). Buckling and post buckling analysis of laminated composite plates in hygrothermal environment using an Inverse Hyperbolic Shear Deformation Theory. *Composite Structures,* 129, 250-255.

Stürzenbecher R, Hofstetter K (2011). Bending of cross-ply laminated composites: An accurate and efficient plate theory based upon models of Lekhnitskii and Ren. *Composite Structures,* 93(3), 1078-1088.

Thai HT, Choi DH (2013a). A simple first-order shear deformation theory for laminated composite plates. *Composite Structures,* 106, 754-763.

Thai HT, Choi DH (2013b). A simple first-order shear deformation theory for the bending and free vibration analysis of functionally graded plates. *Composite Structures,* 101, 332-340.

Vescovini R, Dozio L (2016). A variable-kinematic model for variable stiffness plates: Vibration and buckling analysis. *Composite Structures,* 142, 15-26.

Yin S, Hale JS, Yu T, Bui TQ, Bordas SP (2014). Isogeometric locking-free plate element: a simple first order shear deformation theory for functionally graded plates. *Composite Structures,* 118, 121-138.

Yu T, Bui TQ, Yin S, Doan DH, Wu C, Van Do T, Tanaka S (2016). On the thermal buckling analysis of functionally graded plates with internal defects using extended isogeometric analysis. *Composite Structures,* 136, 684-695.

Zenkour A (2011). Bending responses of an exponentially graded simply-supported elastic/viscoelastic/elastic sandwich plate. *Acta Mechanica Solida Sinica,* 24(3), 250-261.

Zenkour A, Fares M (1999). Non-homogeneous response of cross-ply laminated elastic plates using a higher-order theory. *Composite Structures,* 44(4), 297-305.

Zenkour AM, Allam M, Mashat D (2007). Linear bending analysis of inhomogeneous variable-thickness orthotropic plates under various boundary conditions. *International Journal of Computational Methods,* 4(03), 417-438.

Zerin Z, Turan F, Basoglu MF (2016). Examination of non-homogeneity and lamination scheme effects on deflections and stresses of laminated composite plates. *Structural Engineering and Mechanics,* 57(4), 603-616.

Zhen W, Lo S (2015). Hygrothermomechanical effects on laminated composite plates in terms of a higher-order global-local model. *Journal of Thermal Stresses,* 38(5), 543-568.